Available online at www.sciencedirect.com
SCIENCE DIRECT®
Polymer 45 (2004) 3855–3865
polymer
www.elsevier.com/locate/polymer

Three-dimensional modeling of squamous cell carcinoma antigen 2 and its interactions with serine protease

Xue-feng Gao, Xu-ri Huang*, Jian-kang Yu, Xi Zhao, Chia-chung Sun

State Key Laboratory of Theoretical and Computational Chemistry, Institute of Theoretical Chemistry, Jilin University, Changchun 130023, People's Republic of China

Received 3 March 2004; received in revised form 15 March 2004; accepted 15 March 2004

Abstract

An attempt is made to build up a three-dimensional model of squamous cell carcinoma antigen 2 (SCCA2) by means of the homology module of Insight II, where SCCA2 contains the stressed and relaxed forms, i.e. SCCA2(S) and SCCA2(R). The docking of SCCA2(S) with two different target serine proteinases, that are the cathepsin G (Cat G) and the human mast cell chymase (HMC), are studied theoretically to give two different complexes, respectively. It is shown, from the molecular surface electricity potential, that in the formation of the two complexes SCCA2(S)–Cat G and SCCA2(S)–HMC, the electrostatic interaction may play an important role. Since HMC possesses a loop to produce spatial anti-effect, the complex SCCA2(S)–HMC is less stable than the complex SCCA2(S)–Cat G. However, the reactive site loop involved in SCCA2(S) is an important factor in restraining serine proteinases.

Keywords: Homology modeling; Docking; Hydrophobic interactions

1. Introduction

As is well-known, the squamous cell carcinoma antigen (SCCA) that contains the isoforms SCCA1 and SCCA2 serves as a serological maker for more advanced squamous cell tumors [1,2]. SCCA is not specific for malignant tissues, however, as the protein(s) is detected in the suprabasal levels of normal stratified squamous epithelia of the skin and mucus membranes [3,4] and in the pseudostratified ciliated columnar epithelia of the conducting airways. The functional role of SCCA in both normal and malignant cells has not been elucidated. Biochemical analysis of SCCA by sodium dodecyl sulfate-polyacrylamide gel electrophoresis (SDS-PAGE), reveals a single band with a molecular mass of ~45 kDa [5]. Chromatofocusing, however, separates SCCA into neutral ($pI \geq 6.25$) and acidic ($pI \leq 6.25$) fractions (Table 1) [4,5]. The neutral isoform of SCCA is detected in both malignant and normal epithelial cells [4,6]. Recently, the pioneer work, reported that the SCCA2 was a novel serpin that inhibited the chymotrypsin-like proteinases, cathepsin G (Cat G)[1] and human mast cell chymase (HMC) [7]. To the best of our knowledge, little attention has been paid to the theoretical study on the three-dimensional modeling of SCCA2. In order to make a deeper understanding of SCCA2 at molecular level, an attempt is made in this paper to build up a three-dimensional model of SCCA2 by means of the homology module of Insight II, and further to study the interaction of SCCA2 with the target serine proteinase. The theoretical result may be helpful for the future inhibitor study.

2. Theory and methods

2.1. Three-dimensional modeling of SCCA2

Models of the three-dimensional structure of SCCA2

Abbreviations: SCCA, squamous cell carcinoma antigen; Cat, G, cathepsin G; HMC, human mast cell chymase; RSL, reactive site loop; SDS-PAGE, sodium dodecyl sulfate-polyacrylamide gel electrophoresis; PDB, protein data bank; S, stressed conformation; R, relaxed conformation; RMSD, root mean square deviation; MDS, molecular dynamics simulations.

* Corresponding authors. Tel.: +86-431-8922331; fax: +86-431-8945942.
E-mail address: gaoxuefeng@email.jlu.edu.cn (X. Huang).

[1] The details of Cat G from the human are from Protein Data Bank (ID: 1KYN); details of HMC from the human are from Protein Data Bank (ID: 1NN6).

0032-3861/$ - see front matter © 2004 Elsevier Ltd. All rights reserved.
doi:10.1016/j.polymer.2004.03.039

Table 1
Different amino acid residues of SCCA1 and SCCA2

Basic → basic	Basic → acid	Neutral → acid	Basic → neutral	Acid → neutral	Neutral → basic	Neutral → neutral
Arg321* → His321 His364* → Cys364	Glu165* → Asp165	Gly68* → Glu68 Asn171* → Asp171 Gly353* → Glu353	Lys54* → Ser54 Lys188* → Asn188 His220* → Asn220 Arg279* → Cys279	Asp194* → Asn194 Asp306* → Asn306	Asn191* → Lys191 Gly327* → Lys327	Leu114* → Gln114 Ile163* → Phe163 Asn167* → Thr167 Ser170* → Asn170 Ile210* → Val210 Thr217* → Asn217 Ser223* → Leu223 Val289* → Met289 Gly319* → Gtrp319 Val324* → Ser324 Leu325* → Val325 Ala341* → Val341 Ala351* → Val351 Phe353* → Val351 Ser354* → Leu354 Pro356* → Ser356 Thr357* → Pro357 Val134* → Thr134

*Indicates the amino acid residues of SCCA1.

were carried out on a Silicon Graphics workstation using the Insight II software package. The Insight II module, homology [8], is used for the homology modeling of SCCA2 to give two different elementary models, i.e. the relaxed and stressed models (relaxed and stressed to be abbreviated as R and S). Homology operates by copying coordinates of the backbone atoms from the template molecule to the model and adding the new side chains. Structurally conserved regions assigned coordinates from the template molecule to the model, whereas, other regions assigned coordinates as designated loops. The Loop Search function was used to find suitable loops, from protein structures in the protein data bank (PDB) database, which have the correct number of residues and distance to bridge, and in which the adjacent residues have the appropriate conformations. The two crystal structure of proteins inhibitor from homo sapiens, PDB number 7API and 1QLP, was used as the templates for models of R and S conformations [9,10]. In each case, the model was minimized to a root mean square deviation (RMSD) of 0.000001, employing conjugate gradients using the Discover module [11] of Insight II. Subsequently, the accuracy and validity of the models was tested with the Profiles 3D module [13,14] of Insight II, which performs Eisenberg analysis.

2.2. Amino acid sequence alignments

Sequence alignments were prepared using Insight II software from Molecular Simulations Inc. and empirically refined by hand. Subsequently, to accommodate different colors, the alignment presented here was prepared using CLUSTALX software, and edited manually to replicate the structural alignment generated with Insight II.

2.3. Molecular surface electricity potential

By using Delphi module of Insight II, the surface electricity potentials of the two models, SCCA2(R) and SCCA2(S), are investigated [15]. Also under the CVFF [16] force field, the electrostatic interactions of the two models with the targets, Cat G and HMC, are analyzed.

2.4. The docking of SCCA2 with Cat G and HMC

The FTDOCK [17] software is used to perform the docking of SCCA2(S) with Cat G and HMC [18,19]. The procedure of docking of protein pairs is presented such that FTDOCK scans the full translational and rotational space with the aid of a shape-recognition-algorithm that is very similar to that of Katchalski-Katzir et al. [20]. The two molecules are discretized and the correlation of their surfaces calculated by fast Fourier transformation. For the larger molecule SCCA2(S) and the target proteinases, the shape distribution is represented by a value 1 at each atomic position, a value $p < 0$ in the core of the molecule and a value 0 for open space. For the smaller molecule, the distribution is represented by a value 1 at every atomic position. A correlation function is computed as the sum over all grid-points of the product of the two position scores. In this way, a high correlation score can be used to denote a complex with good surface complementarity. If the smaller molecule significantly overlaps with the larger one, the correlation score is negative. In most cases, a zero correlation score means that the molecules are not in contact. After each translational scan, the smaller molecule is rotated about its three Euler angles, until the rotational space has been scanned completely. For an angular resolution of $a = 10$ degree steps, for example, there are 22.105 non-degenerate

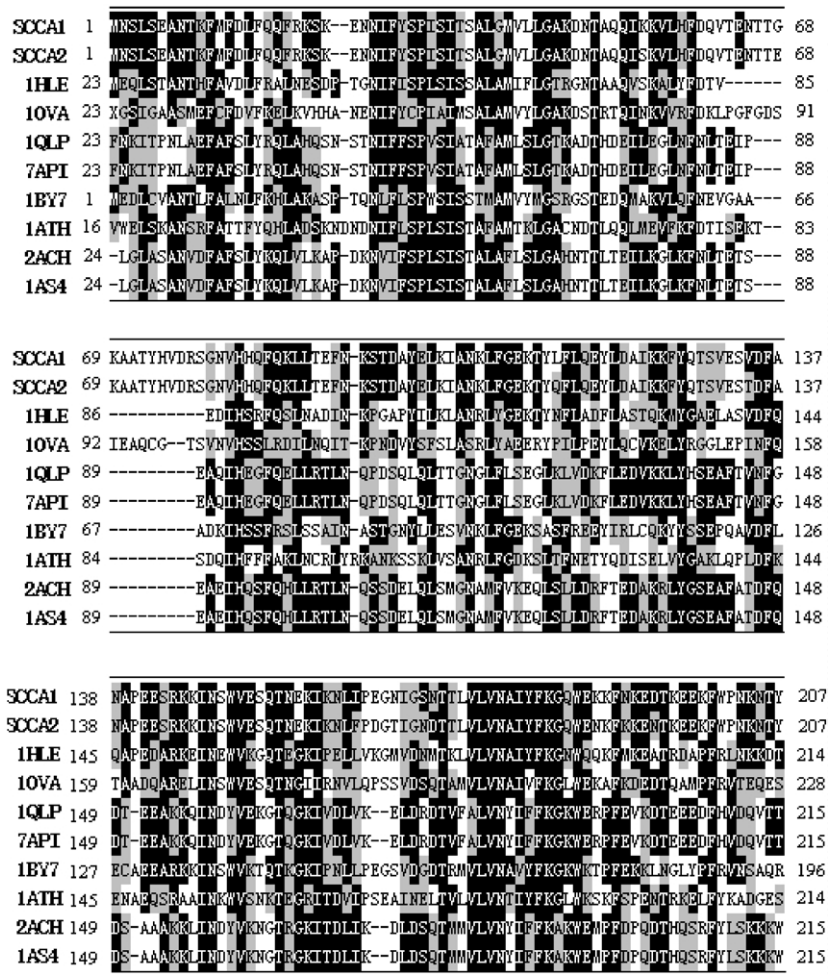

Fig. 1. Sequence alignment of amino acids of nine serpins based on secondary structure and sequence homology. SCCA1: the human squamous cell carcinoma antigen I; SCCA2: The human squamous cell carcinoma antigen II; 1HLE: the horse leukocyte elastase inhibitor; 1OVA: the ovalbumin; 1QLP: the structure of intact alpha-1-antitrypsin A; 7API: the human modified alpha proteinase inhibitor; 1BY7: the human plasminogen activator inhibitor-2; 1ATH: the human antithrombin-III; 2ACH: the human alpha1 antichymotrypsin; 1AS4: the human cleave antichymotrypsin A349R. Black boxes with white letters show identical residues, and gray boxes with black letters show chemically similar residues.

orientations. A simple Coulombic model is then used as a binary filter, leaving only those complexes with attractive electrostatic interactions. Out of these remaining complexes, a large chosen number of complexes are recorded to file. To reduce the number of complexes to a manageable scope, postprocessing consists of a filtering procedure in which the distance constraints are applied to the residues that are known to be part of the docking site through experimental investigations. The distance constraint applied requires the separation between the following residues and protein chains to be <5.0 Å (A and B denote Cat G and HMC, and I stands for SCCA2(S))

(1) the configuration of the complex SCCA2(S)–Cat G I354:A195 I355:A195 I354:A57 I355:A57
(2) the configuration of the complex SCCA2(S)–HMC I354:B197 I355:B197 I354:B60 I355:B60.

2.5. Molecular mechanics optimization of the complexes

Because the FTDOCK [17] is the program of protein–protein rigid docking, it pays no attention to flexibility of protein and solvation. Thereby, we embed the complexes in solvation box, where the radius 10 Å of binding interface of complexes is considered as flexible and the other parts of complexes are considered as rigid. Then, by means of the discover module [11] of insight II, the molecular mechanics optimization is used to perform the energy minimization.

2.6. Molecular dynamics simulations of the complexes

We embed the two complexes, which finally issue for FTDOCK, in solvation box, where the radius 10 Å of binding interface of the complexes is considered as flexible, and the other parts of the complexes are considered as rigid. Then

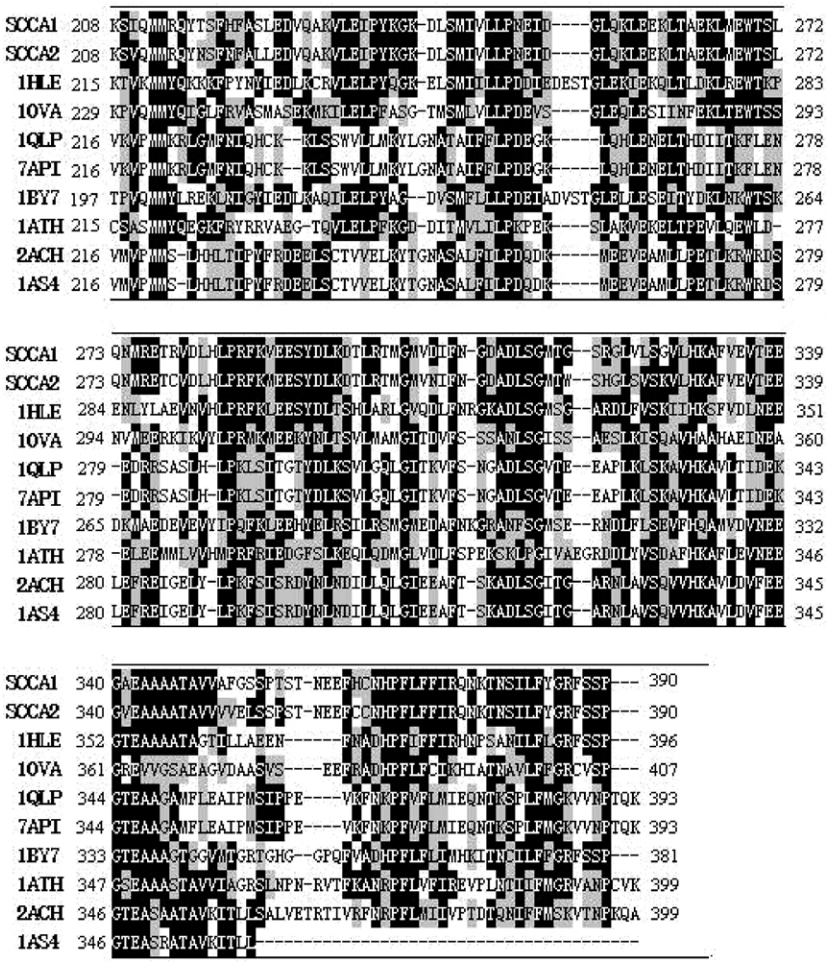

Fig. 1 (*continued*)

by means of the Discover3 [12] module of insight II, the molecular dynamics simulations (MDS) are performed at 300 K for whole system with time of 100 ps. Average structures from MDS are minimized to a RMSD of 0.000001 with the use of conjugate gradients in the Discover [11] module of Insight II.

2.7. The interactions of SCCA2 with Cat G and HMC in the complexes

By means of LIGPLOT [21] software, the hydrogen bonding and the hydrophobic interaction in the complexes SCCA2(S)–Cat G and SCCA2(S)–HMC are studied.

3. Results and discussion

By taking the advantage of being able to use the identity of homologous sequence, it is not difficult to find that, for the elementary SCCA2 model and the corresponding template, the sequence identity is about 33%. From the sequence similarity, the sequence alignment of amino acids for nine serpins based on secondary structure and the sequence homology are established as shown in Fig. 1, where the black boxes with the white letters show the conserved amino acid residues, and the grey boxes with the black letters the chemically similar residues, and the broken lines the deletion. Furthermore, Profiles 3D [13,14] is used to analyze the conformations of SCCA2(R) and SCCA2(S) to give the scores of 188 and 164, respectively, compared with the overall self-compatibility scores of 198 and 177, and the lowest possible scores of 89 and 80. These (188 and 164) are the high figures, indicating the high probabilities that the models are correct.

Let us discuss the conformations of SCCA2(R) and SCCA2(S). Fig. 2(a) and (b) show the most preferential conformations of SCCA2(R) and SCCA2 (S) and these conformations possess the common structural characteristics to have rich α-helices and β-sheets. For SCCA2(S), the c-terminal has a loop referred to as reactive site loop (RSL). The RSL of serpins interacts with the active site of the proteinase, and thereby, confers both functionality and specificity to the serpin molecule [22–25]. When the RSL of serpins interact with the active sites of the proteinases, it

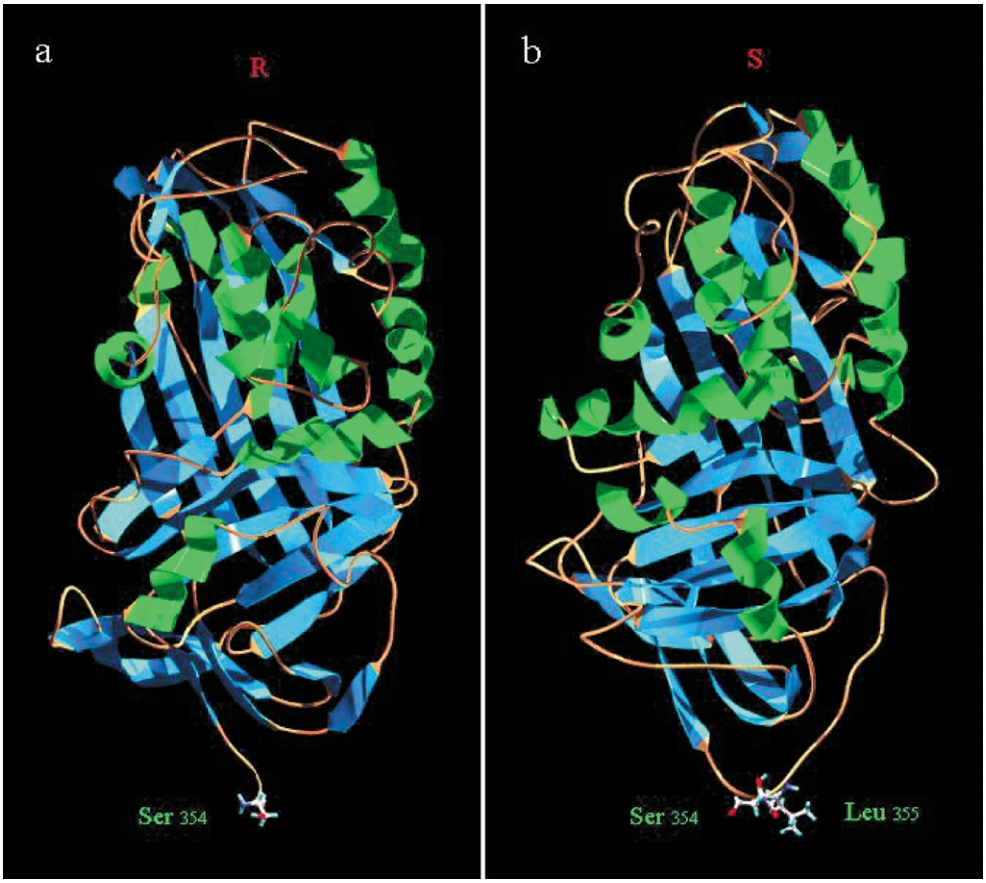

Fig. 2. The conformations of the SCCA2(R) and SCCA2(S). The R and S conformations display using the Swiss-PdbViewer and POV-Ray for Windows program. Helices are green and sheets are Cambridge blue, random coil are orange yellow. Ball–stick are residues of active site. (a) The conformations of SCCA2(R). (b) The conformations of SCCA2(S).

is likely to produce the complexes SCCA2(S)–Cat G and SCCA2(S)–HMC, and to make SCCA2(S) as an inhibitor to restrain both the active centers of Cat G and HMC. The details will be discussed in later sections by the use of Tables 2 and 3 as well as Figs. 5 and 6. Moreover, the residues flanking at the putative scissile bonds in RSLs, between P1 and P19 residues [26] according to the numbering system of Schechter and Berger, are Leu^{354}…Ser^{355} [27].

For the comparison of RSLs in serpin, Fig. 3 shows the position of the scissile bond that can make RSL separate from SCCA2(S), where the triangle indicates that the scissile bond appears in the range (Leu^{354}…Ser^{355}). Furthermore, when serpin binds with Ser, it is broken at P1, and the c-terminal of the broken peptide extends into a sheet to make new six sheets formed from the old five sheets. As a result, it is likely that the conformation of SCCA2(S) may change from the stressed form to the relaxed SCCA2(R). Table 4 shows the CVFF energies for SCCA2(R) and SCCA2(S), in which the electrostatic, the Van der Waals and the hydrogen bond energies are involved. Since the Van der Waals and the hydrogen bond energies of SCCA2(R) is lower than that of SCCA2(S), this informs, from the thermodynamics stability, that the conversion of SCCA2(R) into SCCA2(S) is reasonable.

The surface electrostatic potentials of SCCA2, Cat G and

Table 2
The CVFF energies for complexes of SCCA2(S)–Cat G

FTDOCK-score	Elect (kcal/mol)	VDW (kcal/mol)	Total (kcal/mol)	I354–A195 distance (Å)	I355–A57 distance (Å)
9258	−5505.2	338.7	−5166.5	3.7	4.2
8905	−5515.7	350	−5165.7	4.9	4.1
7741	−5496.4	376.3	−5120.1	4.4	3.2
7169	−5518.6	343	−5175.6	3.7	3.8

Elect: electrostatic energy; VDW: Van der Waals energy; total: total energy; I354–A195: distance between the carboxyl of leu^{354} in SCCA2(S) and the hydroxyl of Ser^{195} in Cat G; I355–A57: distance between the amido of Ser^{355} in SCCA2 and sidechain of His^{57} in Cat G.

Table 3
The CVFF energies for complexes SCCA2(S)–HMC

FTDOCK-score	Elect (kcal/mol)	VDW (kcal/mol)	Total (kcal/mol)	I354–A197 distance (Å)	I355–A60 distance (Å)
8712	−2403.5	2276.4	−127.2	4.2	3.5
7380	−2414.2	2318.3	−95.9	4.5	4.1
6487	−2403.0	2298.7	−104.3	4.2	3.7

Elect: electrostatic energy; VDW: Van der Waals energy; total: total energy; I354–A197: distance between the carboxyl of leu^{354} in SCCA2(S) and the hydroxyl of Ser^{197} in Cat G; I355–A60: distance between the amido of Ser^{355} in SCCA2(S) and the sidechain of His^{60} in HMC.

HMC are displayed in Fig. 4. There is a large positive electricity potential region in the solvent surface of Cat G and HMC whose active centers are just in that positive region, but in the solvent surface of SCCA2, the RSL region lies in a large negative electricity potential region. There are some acidic conservative residues such as Glu^{225}, Asp^{226}, Asp^{252}, Glu^{258} and Glu^{264} in the region approaching the RSL region. The symmetric surface electrostatic potential is very common between serpin and serine proteinase just like in SCCA2, Cat G and HMC. Thus, we conclude that what is like the SCCA2–Cat G electrostatic interaction will also occur in HMC during the binding process of protein inhibitor and serine proteinase.

For gain the complex models we used a successful docking strategy in which the reliability of the method. First, under the solvent condition, we optimize conformations of SCCA2, Cat G and HMC. Second, we used FTDOCK [17] program, got a large amount complex structures and during the initial sequence based on distance. Lastly, under the solvent condition, used CVFF [16] force field doing the optimization on the screened

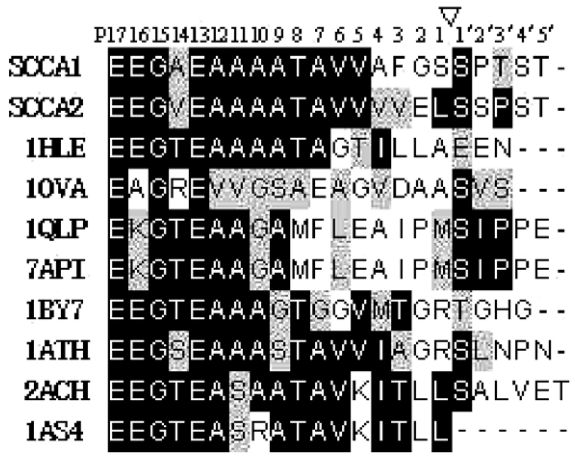

Fig. 3. Comparison of serpin RSLs. Inhibitory and non-inhibitory serpin RSLs from P17-P5′ are aligned using the insight II program. The triangle indicates position of the scissile bond. SCCA1: The human squamous cell carcinoma antigen I; SCCA2: the human squamous cell carcinoma antigen II; 1HLE: the horse leukocyte elastase inhibitor; 1OVA: the ovalbumin; 1QLP: the structure of intact alpha-1-antitrypsin A; 7API: the human modified alpha proteinase inhibitor; 1BY7: the human plasminogen activator inhibitor-2; 1ATH: the human antithrombin-III; 2ACH: the human alpha1 antichymotrypsin; 1AS4: the human cleave antichymotrypsin A349R. Black boxes with white letters show identical residues, and gray boxes with black letters show chemically similar residues.

complex structure, and electing the complex lowest in energy had an RMSD of <2.0 Å compared with the crystal coordinates (C_α-carbon atoms).

For the scanned complex structures, the energies take the minimum values and the distances the smallest ones. In Table 2, the FTDOCK-score 7169 fits the complex SCCA2(S)–Cat G with the minimum energy −517.65 kcal/mol and the smallest distance I354–A195 (3.7 Å), i.e. the distance between the carboxyl of Leu^{354} in SCCA2(S) and the hydroxyl of Ser^{195} as active center in Cat G, where the docking result has been decreased from 1×10^4 to 4 and the RMSD of Cat G of the complex 7169 with respect to the X-ray structure of Cat G is 1.14 Å. Moreover, after MDS for the complexes 7169, the interrelation between RSL in SCCA2(S) and Cat G is drawn schematically in Fig. 5. It is shown that there are three hydrogen bondings between RSL in SCCA2(S) and amino acid residues in the active pocket of Cat G, and also there is one H_2O molecule which forms hydrogen bondings with Ser^{195} as active center in Cat G, and this H_2O molecule could have possibly taken part in the rupture of the acidamide bond between Leu^{354} and Ser^{355}. Note that, in Fig. 5, the distance I354–A195 takes the value 3.97 Å. For brevity, we only state without the details that for the complex, the Pro^{357}, which is near the proteinase, with the noticed point, inserts into the region which is near the Asp^{104}, and it is in accordance to the experiment results [28].

Similarly, as we have done for Table 2 and Fig. 5, Table 3 shows that the FTDOCK-score 8172 fits the complex SCCA2(S)–HMC with the minimum energy −27.2 kcal/mol, and the smallest distance I354–A197 (4.2 Å), i.e. the distance between the carboxyl of Leu^{354} in SCCA2(S) and the hydroxyl of Ser^{197} in HMC, where the docking result as listed in Table 3 has been

Table 4
The CVFF energies for SCCA2(S) and SCCA2(R)

	VDW (kcal/mol)	Elect (kcal/mol)	Hbond (kcal/mol)	Total (kcal/mol)
R conformation	−1301.9	−246.7	−102.3	−1650.9
S conformation	−1022.2	−328.8	−64.9	−1415.9

Elect: electrostatic energy; VDW: Van der Waals energy; Hbond: hydrogen bond energy; total: total energy.

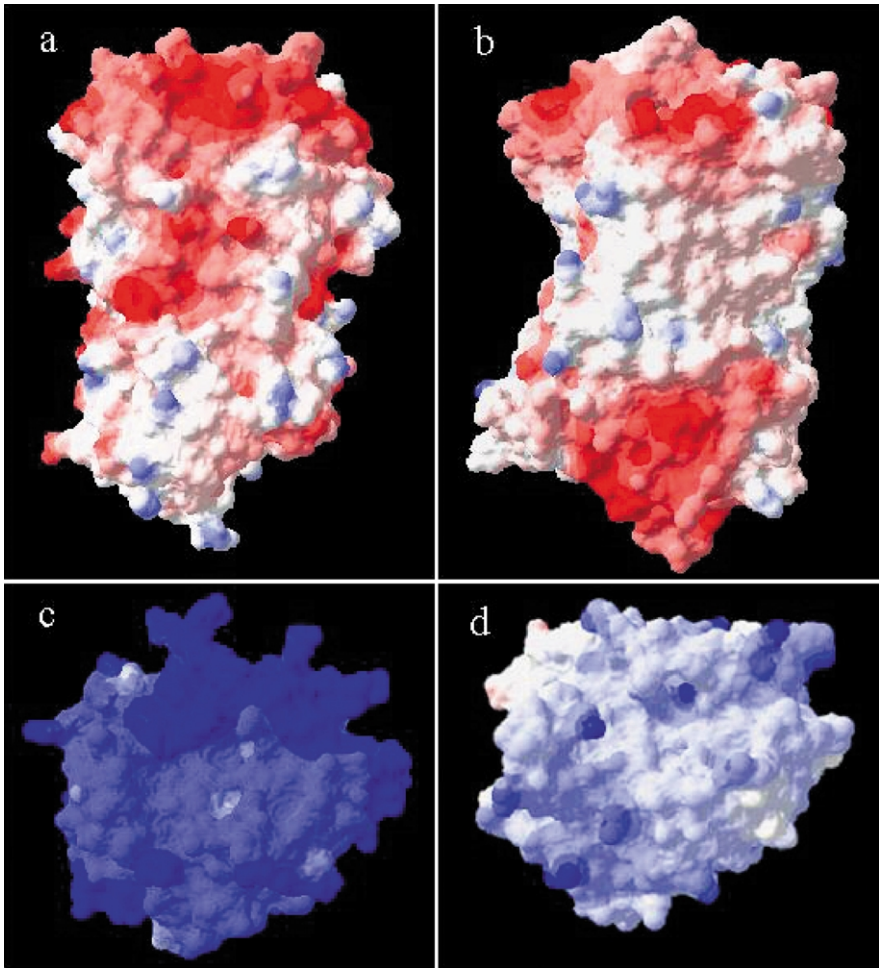

Fig. 4. The surface electricity potential of SCCA2(R), SCCA2(S) with RSL, Cat G and HMC. (a) The surface electricity potential of SCCA2(R); (b) the surface electricity potential of SCCA2(S) with RSL; (c) the surface electricity potential of Cat G; (d) the surface electricity potential of HMC. Positive electricity potential region is blue, negative electricity potential region is red.

Table 5
Comparison of interactions in interface of complexes 7169 and 8712

Complex 7169			Complex 8712		
Cat G	SCCA2	Type of interaction	HMC	SCCA2	Type of interaction
Arg 97*	Ser 358*	Hydrophobic interactions	Pro 41	Val 349	Hydrophobic interactions
Gln 96	Ser 358*	Hydrophobic interactions	Pro 41	Val 352	Hydrophobic interactions
Gln 96	Pro 357	Hydrophobic interactions	Ser 212*	Ser 356*	Hydrogen bond
Ile 99	Ser 357*	Hydrophobic interactions	Asn 39*	Val 352	Hydrophobic interactions
Lys 192*	Val 352	Hydrogen bond	Ile 35	Leu 354	Hydrophobic interactions
Tyr 94*	Ser 356*	Hydrophobic interactions	Lys 43*	Val 352	Hydrophobic interactions
Tyr 215*	Ser 355*	Hydrophobic interactions	Lys 43*	Glu 353*	Hydrophobic interactions
His 57*	Ser 356*	Hydrogen bond	Cys 61*	Leu 354	Hydrophobic interactions
His 57*	Pro 357	Hydrophobic interactions	Phe 44	Leu 354	Hydrophobic interactions
Gly 193	Leu 354	Hydrophobic interactions	His 60*	Pro 357	Hydrophobic interactions
Ser 212*	Val 351	Hydrophobic interactions	Thr 98*	Asp 281*	Hydrophobic interactions
Arg 97	Arg 214	Hydrophobic interactions	Gly 147	Ser 356*	Hydrophobic interactions
Phe 172	Arg 276*	Hydrophobic interactions	Cys 45*	Leu 354	Hydrophobic interactions
Lys 192*	Val 352	Hydrophobic interactions	Leu 101	Pro 357	Hydrophobic interactions
Ser 195*	Ser355*	Hydrogen bond	Thr 98*	Thr 359*	Hydrophobic interactions
			Thr 37*	Val 352	Hydrophobic interactions

*Indicates that the aliphatic portion of this polar sidechain is involved in the hydrophobic pocket.

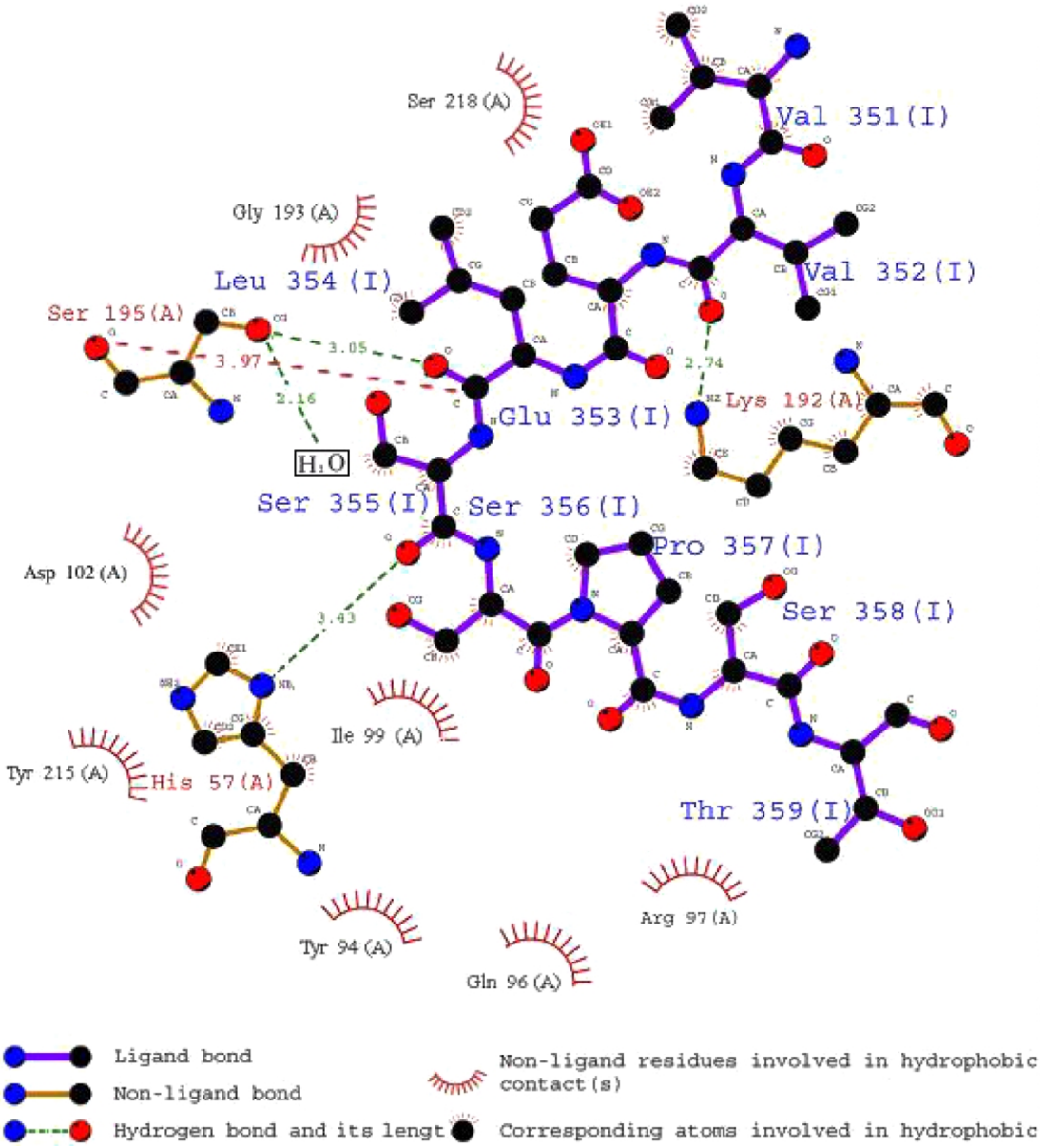

Fig. 5. Schematic drawing of interrelation between Cat G and SCCA2(S) with RSL in complex # 7169. The interrelations using the LIGPLOT program and edited manually. Hydrogen bonds are shown as green dashed lines, distance between the carboxyl of leu^{354} in SCCA2(S) and the hydroxyl of Ser^{195} in Cat G are shown as red dashed lines, and distances are indicated in Å. (For interpretation of the references to color in this figure legend, the reader is referred to the web version of this article.)

decreased from 1×10^4 to 3 and the RMSD of HMC of the complex 8172 with respect to the X-ray structure of HMC is 1.63 Å. Moreover, after MDS for the complexes 8172, the interrelation between RSL in SCCA2(S) and HMC is drawn schematically in Fig. 6. It is shown that there is one hydrogen bonding between Ser^{356} at RSL of SCCA2(S) and Ser^{212} in the active pocket of HMC, and there is one H_2O molecule, which forms one hydrogen bonding with the carboxyl of Ser^{355} in HMC, and this H_2O molecule could have possibly taken part in the rupture of the acidamide bond between Leu^{354} and Ser^{355}. Note that, in Fig. 6, the distance I354–A197 is 4.33 Å. For brevity, we only state without details that for the complex, the Pro^{357}, which is near the proteinase, with the noticed point, inserts into the region which is near the Asp^{104}, and it is in accordance to the experiment results [28].

From the discussion, it is shown, by means of Tables 2 and 3 as well as Figs. 5 and 6, that when the RSL of serpins interact with the active sites of proteinases, it is likely to produce the complexes SCCA2(S)–Cat G and SCCA2(S)–HMC, and to make SCCA2(S) as an inhibitor to restrain both the active centers of Cat G and HMC.

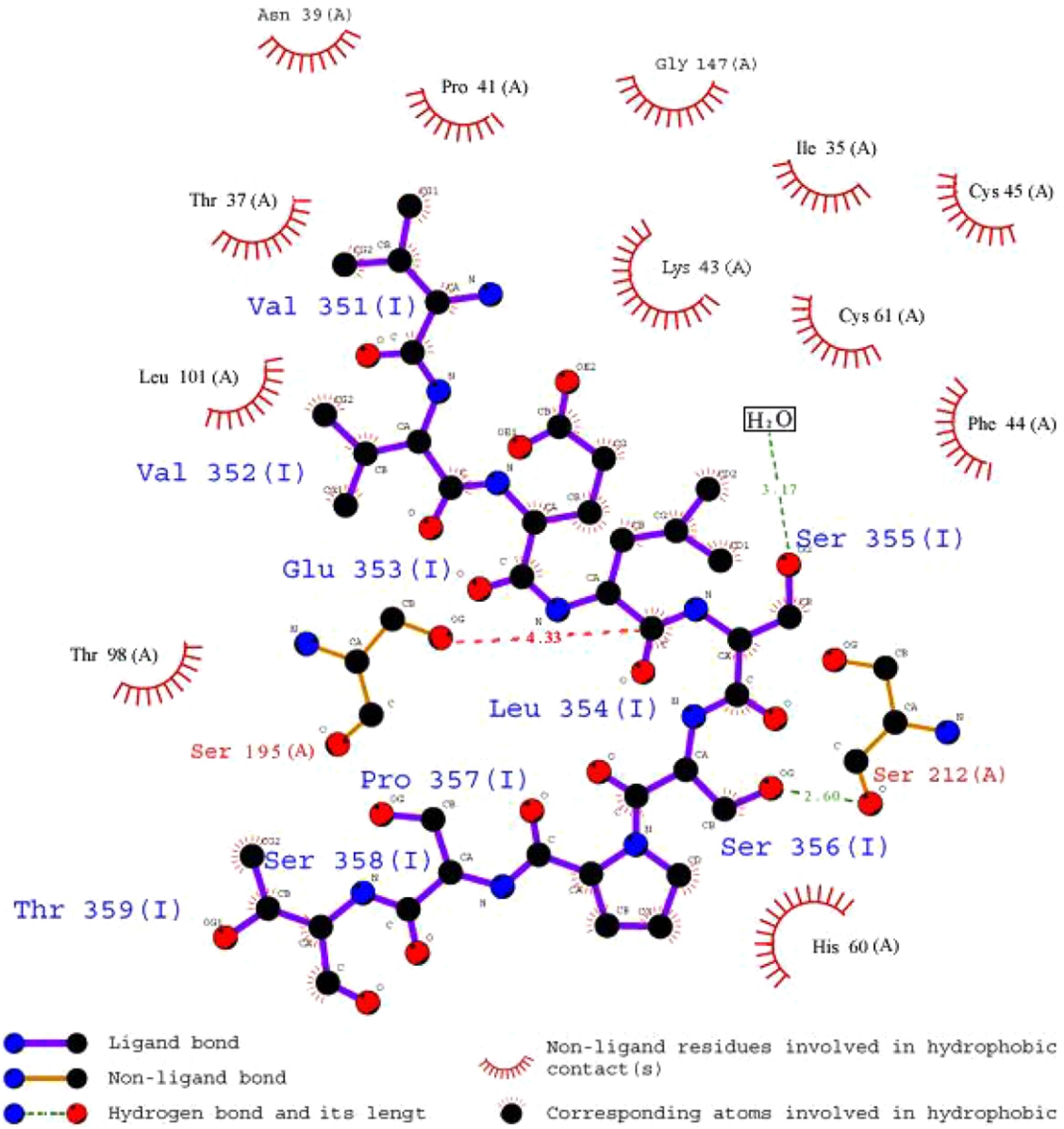

Fig. 6. Schematic drawing of interrelation between HMC and SCCA2(S) with RSL in complex # 8712. The interrelations using the LIGPLOT program and edited manually. Hydrogen bonds are shown as green dashed lines, distance between the carboxyl of leu^{354} in SCCA2(S) and the hydroxyl of Ser^{197} in HMC are shown as red dashed lines, and distances are indicated in Å. (For interpretation of the references to color in this figure legend, the reader is referred to the web version of this article.)

The important contacts between SCCA2(S) and Cat G (HMC) in complex 7169 and 8712 are shown in Table 5. The different contacts in the interfaces involving the complexes 7169 and 8712 may be closely related with the stabilities of the complexes. It is shown that, for the complex 7169, SCCA2(S)–Cat G, there are, between SCCA2(S) and Cat G, 3 hydrogen bondings and 12 hydrophobic interactions, whereas, for the complex 8712, SCCA2(S)–HMC, there are, between SCCA2(S) and HMC, 15 hydrophobic interactions and only one hydrogen bonding, so that the complex 7169 is likely to be more stable than the complex 8712. It is plausible to predict that the reaction rate for SCCA2(S) with Cat G is faster than that for SCCA2(S) with HMC. This prediction is in harmony with the experimental reaction rates for SCCA2(S) with Cat G and HMC, i.e. $1 \times 10^5\ M^{-1}\ S^{-1}$ and $3 \times 10^4\ M^{-1}\ S^{-1}$ [7].

In obtaining the three-dimensional structures of Cat G and HMC, the computational process leads to, that Cat G and HMC have the RMSD 0.92 Å. However, the main difference between the conformations of Cat G and HMC as shown in Fig. 7 is that HMC has a loop (Gly^{144} to Asp^{154}) extended to overlap with the upper part of the active center, and this loop produces spatial anti-effect, so that the complex SCCA2(S)–HMC is less stable than the complex SCCA2(S)–Cat G.

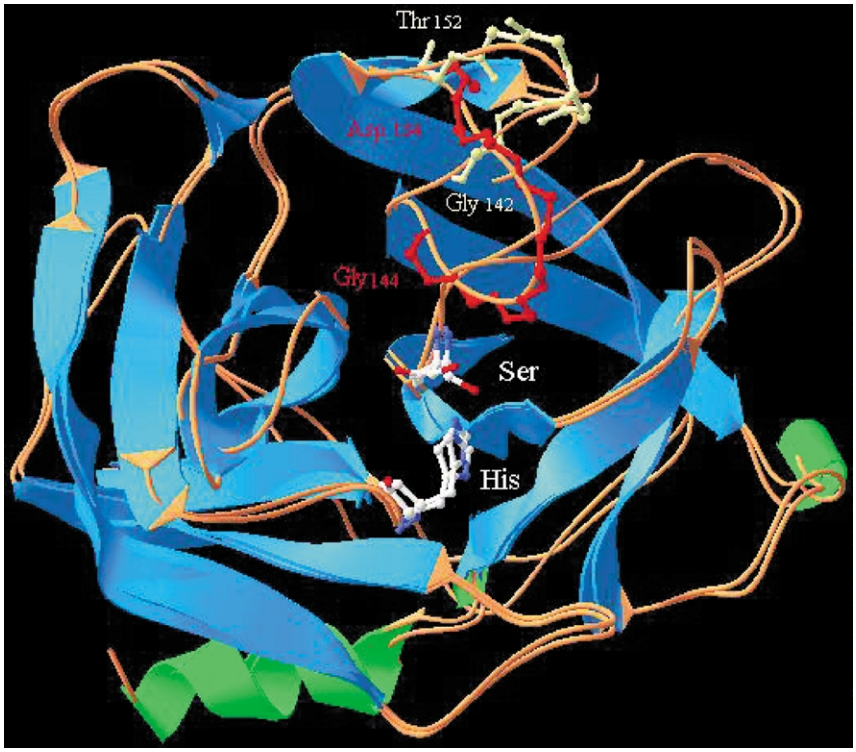

Fig. 7. Schematic drawing of comparison conformations of Cat G and HMC. The loop (Gly142-Thr152) of Cat G is buff and the loop (Gly144-Asp154) of HMC is red. Helices are green and sheets are Cambridge blue, random coil are orange yellow. The ball–stick are residues (His and Ser) of active site.

Acknowledgements

This work is supported by provincial technology development plan of Jilin.

References

[1] Kato H, Torigoe T. Radioimmunoassay for tumor antigen of human cervical squamous cell carcinoma. Cancer 1977;40:1621.
[2] Kato H. In: Sell S, editor. Serological cancer markers. Totowa, NJ: Humana Press; 1992. p. 437.
[3] Takeshima N, Suminami Y, Takeda O, Abe H, Okuno N, Kato H. Expression of mRNA of SCC antigen in squamous cells. Tumour Biol 1992;13:338.
[4] Kato H, Suehiro Y, Morioka H, Torigoe T, Myoga A, Sekiguchi K, Ikeda I. Heterogeneous distribution of acidic TA-4 in cervical squamous cell carcinoma: immunohistochemical demonstration with monoclonal antibodies. Jpn J Cancer Res 1987;78:1246.
[5] Kato H, Nagaya T, Torigoe T. Heterogeneity of a tumor antigen TA-4 of squamous cell carcinoma in relation to its appearance in the circulation. Gann 1984;75:433.
[6] Mueller PR, Wold B. In vivo footprinting of a muscle specific enhancer by ligation mediated PCR. Science 1989;246:780.
[7] Schick C, Kamachi Y, Bartuski AJ, Çataltepe S, Schechter NM, Pemberton PA, Silverman GA. Squamous cell carcinoma antigen 2 is a novel serpin that inhibits the chymotrypsin-like proteinases cathepsin G and mast cell chymase. J Biol Chem 1997;272:1849.
[8] Homology user guide, MSI, San Diego, USA; 1999.
[9] Needleman SB, Wunsch CD. A general method applicable to the search for similarities in the amino acid sequence of two proteins. J Mol Biol 1970;48:443.
[10] Engh R, Lobermann H, Schneider M, Wiegand G, Huber R, Laurell CB. The S variant of human alpha 1-antitrypsin, structure and implications for function and metabolism. Protein Engng 1989;2:407.
[11] Discover user guide, MSI, San Diego, USA; 1999.
[12] Discover 3 user guide, MSI, San Diego, USA; 1999.
[13] Profile-3D Uesr Guide, MSI, San Diego, USA, 1999.
[14] Luthy R, Bowie JU, Eisenberg D. Assessment of protein models with three-dimensional profiles. Nature 1992;356:83.
[15] Delphi user guide, MSI, San Diego, USA; 1999.
[16] CVFF user guide, MSI, San Diego, USA; 1999.
[17] Gabb HA, Jackson RM, Sternberg MJ. Modelling protein docking using shape complementarity, electrostatics and biochemical information. J Mol Biol 1997;272:106.
[18] Greco MN, Hawkins MJ, Powell ET, Almond Jr HR, Corcoran TW, De Garavilla L, Kauffman JA, Recacha R, Chattopadhyay D, Andrade-Gordon P, Maryanoff BE. Nonpeptide inhibitors of cathepsin G. optimization of a novel beta-ketophosphonic acid lead by structure-based drug design. J Am Chem Soc 2002;124:3810.
[19] Reiling KK, Krucinski J, Miercke LJ, Raymond WW, Caughey GH, Stroud RM. Structure of human pro-chymase: a model for the activating transition of granule-associated proteases. Biochemistry 2003;42:2616.
[20] Katchalski-Katzir E, Shariv I, Eisenstein M, Friesem AA, Aflalo C, Vakser IA. Molecular surface recognition: determination of geometric fit between proteins and their ligands by correlation techniques. Proc Natl Acad Sci USA 1992;89:2195.
[21] Wallace AC, Laskowski RA, Thornton JM. LIGPLOT: a program to generate schematic diagrams of protein–ligand interactions. Protein Engng 1995;8:127.
[22] Travis J, Salvesen GS. Human plasma proteinase inhibitors. Annu Rev Biochem 1983;52:655.

[23] Carrell RW, Aulak KS, Owen MC. The molecular pathology of the serpins. Mol Biol Med 1989;6:35.
[24] Francke U. High-resolution ideograms of trypsin-Giemsa banded human chromosomes. Cytogenet Cell Genet 1981;31:24.
[25] Travis J, Guzdek A, Potempa J, Watorek W. Serpins: structure and mechanism of action. Biol Chem Hoppe–Seyler 1990;371:3.
[26] Schechter I, Berger A. On the size of the active site in proteases. I. Papain. Biochem Biophys Res Commun 1967;27:157.
[27] Schneider SS, Schick C, Fish KE, Miller E, Pena JC, Treter SD, Hui SM, Silverman GA. A serine proteinase inhibitor locus at 18q21.3 contains a tandem duplication of the human squamous cell carcinoma antigen gene. Proc Natl Acad Sci USA 1995;92:3147.
[28] Reiling KK, Krucinski J, Miercke LJ, Raymond WW, Caughey GH, Stroud RM. Structure of human pro-chymase: a model for the activating transition of granule-associated proteases. Biochemistry 2003;42:2616.